GA–A22342

DiMES DIVERTOR EROSION EXPERIMENTS ON DIII–D

by

D.G. WHYTE, J.N. BROOKS, C.P.C. WONG, W.P. WEST,
R. BASTASZ, W.R. WAMPLER, and J. RUBINSTEIN

MAY 1997

GA–A22342

DiMES DIVERTOR EROSION EXPERIMENTS ON DIII–D

by
D.G. WHYTE,[†] J.N. BROOKS,[‡] C.P.C. WONG, W.P. WEST,
R. BASTASZ,[◊] W.R. WAMPLER,[◊] and J. RUBINSTEIN[Δ]

This is a preprint of a paper to be presented at the 12th International Conference on Plasma Surface Interactions on Controlled Fusion Devices, May 20–24, 1996, Saint-Raphael, France and to be published in the *Proceedings*.

[†]INRS—Energie et Materiaux, Varennes, Quebec, Canada
[‡]Argonne National Laboratory, Argonne, Illinois
[◊]Sandia National Laboratories, Albuquerque, New Mexico
[Δ]University of Illinois, Urbana, Illinois

Work supported by
the U.S. Department of Energy
under Contract Nos. DE-AC03-89ER51114, W-31-ENG-38,
and DE-AC04-94AL85000

GA PROJECT 3469
MAY 1997

ABSTRACT

The DiMES (Divertor Material Evaluation Studies) mechanism allows insertion of material samples to the lower divertor floor of the DIII–D tokamak. The main purpose of these studies is to measure erosion rates and redeposition mechanisms under tokamak divertor plasma conditions in order to obtain a physical understanding of the erosion/redeposition processes and to determine its implications for fusion power plant plasma facing components. Thin metal films (~100 nm thick) of Be, W, V, and Mo, were deposited on a Si depth-marked graphite sample and exposed to the steady-state outer strike point (0.7 MW/m^2, ELM-free H–mode) on DIII–D. A variety of surface analysis techniques (NRA, RBS) are used to determine the erosion/redeposition of the metals and the carbon after 5–15 s of exposure. These short exposure times ensure controlled exposure conditions and the extensive array of DIII–D divertor diagnostics provide a well characterized plasma for modeling efforts. Erosion rates and redeposition lengths are found to decrease with the atomic number of the metallic species, as expected. Under these conditions, the peak net erosion rate for carbon is ~4 nm/s, with the erosion following the ion flux profile. Comparisons of the measured carbon erosion with REDEP code calculations show good agreement for both the absolute net erosion rate and its spatial variation. Measured erosion rates of the metals are smaller (factor of ~4 for Be) than predicted for sputtering from a bare metal surface, apparently due to effects of carbon deposition on the metal surface.(post-exposure carbon layer $\gtrsim$1 nm). Visible spectroscopic measurements of singly ionized Be (BeII 4674 Å) have determined that the erosion process reaches steady-state during the exposure. Calculations of the Be II line integrated brightness using a Monte-Carlo code (WBC) independently verify the erosion rates measured by the surface analysis techniques within a factor of 2. Additional exposures of Be/W films at higher particle and heat flux (2 MW/m^2, ELMing H–mode) will determine the scaling of erosion rates and redeposition properties with heat flux and the effect of ELMs.

1. INTRODUCTION

The Divertor Material Evaluation Studies (DiMES) [1] program on the DIII–D tokamak is being used to measure erosion characteristics of Carbon and several candidate plasma facing metals (Beryllium, Tungsten, Vanadium and Molybdenum). Samples are exposed to steady-state outer strike point plasmas for durations ranging from 4–18 s. Pre and post-exposure analysis of the samples using ion beam analysis techniques have previously measured [2,3] the erosion rates and redeposition profiles of the metallic films onto the surrounding carbon under ELM-free conditions at modest heat flux (0.7 MW/m^2). Also the net erosion profile of the intrinsic carbon and the deuterium retention of the materials were measured. We report here additional analysis from these exposures as well as the results of the initial effort of scaling the erosion characteristics of these materials to higher incident heat flux (2 MW/m^2).

2. EXPERIMENT

2.1. APPARATUS AND PLASMA DIAGNOSTICS

The DiMES mechanism [Fig. 1(a)] allows for the insertion and retraction of test samples to the DIII–D divertor floor. The 4.7 cm diameter sample is aligned to the surrounding graphite tiles to within 0.25 mm vertical distance and 0.1 degrees horizontal orientation. The relative heights of the surrounding tiles referenced to the DiMES surface are indicated in Fig. 1(b). Note that the misalignment is maximum in the downstream, inboard direction from the sample.

The divertor plasma is well characterized by a series of diagnostics. Dedicated non-exposure discharges in which the plasma outer strike point (OSP) is slowly varied over 8 cm are used to obtain radial profiles of the ion flux, electron temperature and density from the fixed floor Langmuir probes and divertor Thomson scattering. Heat flux radial profiles on the floor tiles are derived from infrared thermography. A visible spectrometer directly views the DiMES sample [Fig. 1(b)]. A CCD camera, which can be equipped with interference line filters, views DiMES and the surrounding tiles. Magnetic geometry, including the position of the separatrix and the magnetic field pitch angle, are derived from the magnetic reconstruction code EFIT.

The samples consist of ATJ-type graphite, polished to a 0.25 μm finish on their plasma facing side. The depth marking technique [2] allows measurement of the net carbon erosion/redeposition to ± 10 nm with 1mm lateral spatial resolution. Thin uniform films (100 nm thickness) of metals are deposited on the graphite via electron beam evaporation deposition. The sample designated as DiMES 71 (70) has alternating squares (7.5 × 7.5 mm) of Be and W (V and Mo) spaced radially at the toroidal center of the sample. The DiMES 74 sample has a radial stripe (3 mm × 32 mm) of W offset 10 mm upstream and one of Be offset 10 mm downstream [Fig. 1(b)] from the sample's toroidal center.

2.2. SAMPLE EXPOSURES

The desired plasma is achieved with the OSP positioned outside of the DiMES major radius (R=1.484 m), leaving the sample practically unexposed to plasma interaction until the OSP is programmed to move onto the sample. This ensures that the sample's exposure conditions are steady-state. Figure 2 shows the time traces for two of the exposure discharges of DiMES 74. Note the reproducibility of the peak heat flux, the plasma positioning and the Be II line brightness. In particular, the Be II brightness, which to a first approximation is

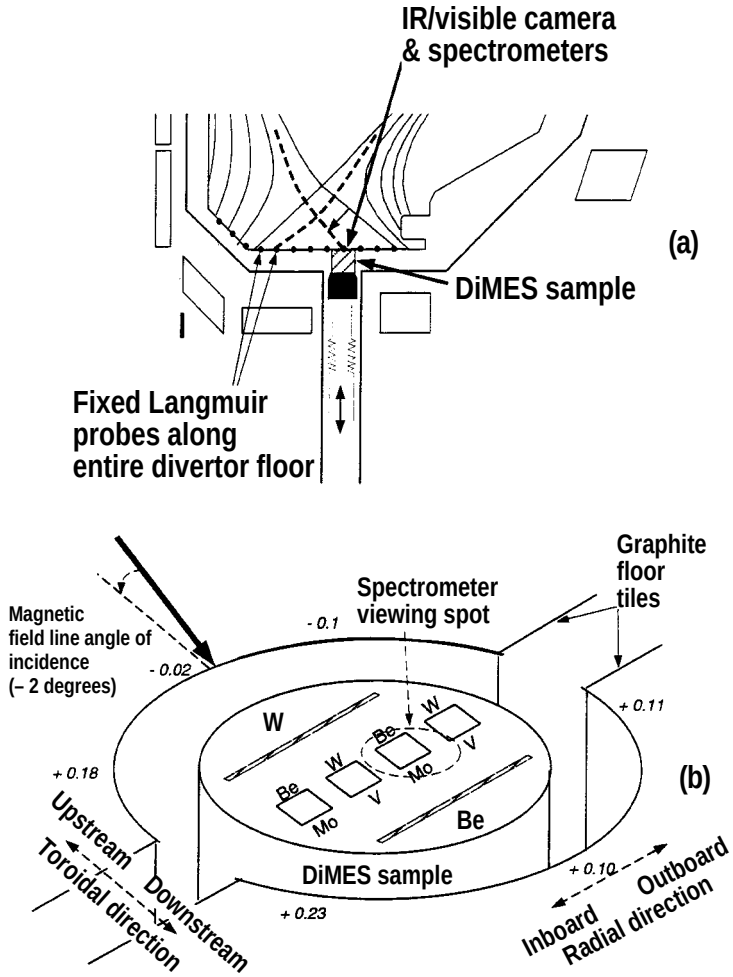

Fig. 1. (a) Poloidal cross-section of DiMES exposure. Sample is kept in private flux region until OSP is swept onto probe (dashed flux lines).(b) DiMES sample, metallic films and surrounding graphite tile geometry. Numbers indicate relative height of tiles to standard DiMES surface in mm. The gap between the sample and tiles is exaggerated for viewing clarity.

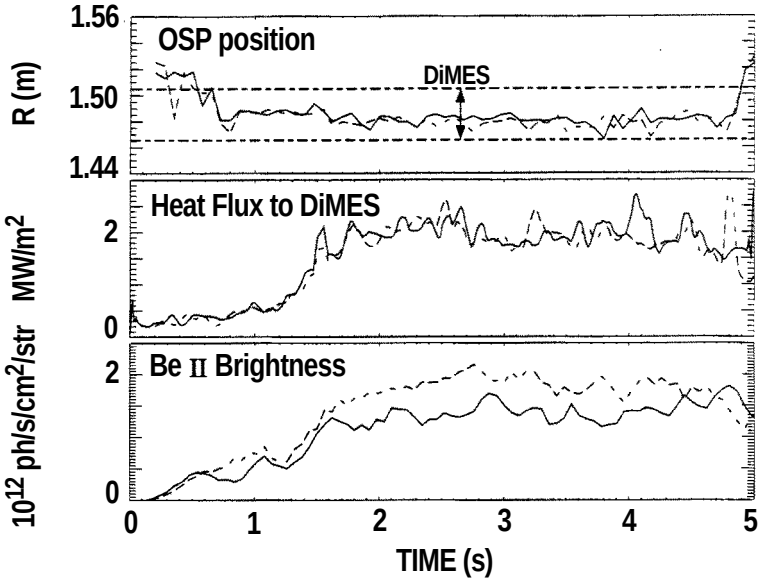

Fig. 2. Time traces of OSP postion, heat flux and Be II (4673 Å) brightness for first and third of the four DiMES 74 exposure discharges (solid line: #86987, dashed line: #86989).

determined by the beryllium flux into the plasma for a fixed divertor plasma, indicates that the erosion of the beryllium film is a continuous process. Typically, the positioning control of the separatrix on the sample is accurate to within 5 mm. Other global plasma parameters of interest are: gas=D_2, I_p=1.35–1.4 MA, B_T= –1.9 T, magnetic pitch angle at OSP=1.5°–2.5°, Z_{eff}=1.5, carbon fraction in core= 1%–2 %, oxygen fraction in core=0.1%–0.2 %.

Keeping these plasma parameters as constant as possible the neutral beam injection power was increased from 2.5 MW (for DiMES 70&71 exposures, hereby designated as DiMES 70) to 7.5 MW (DiMES 74). Table 1 indicates the variation in the OSP quiescent plasma parameters between the two conditions.

Table 1
Divertor Plasma Parameters for Exposures

OSP parameter	ELMing	Heat Flux (MW/m^2)	Incident Ion Flux [$s^{-1}m^{-2}$]	n_e [m^{-3}]	T_e [eV]
DiMES 70	No	0.7	3×10^{22}	4×10^{19}	70
DiMES 74	Yes	2.0	9×10^{22}	1.0×10^{20}	45

2.3. EROSION AND REDEPOSITION RESULTS

Ion beam analysis is performed on the samples before and after exposure. Rutherford Backscattering Spectroscopy (RBS) provides the relative changes in the Si marker depth for carbon erosion and the effective areal concentrations for the high-Z metals (V,Mo,W). Nuclear Reaction Analysis (NRA) is used to determine the Be concentration via the $^9Be(p,\alpha)^6Li$ reaction. These measurements have a lateral spatial resolution of 1 mm, determined by the ion beam's dimension. The metallic erosion rates are derived either directly from decreases in the areal concentration of the metal films or from the integrated quantity of redeposited metal on the surrounding graphite of the DiMES sample. Figure 3 shows the post-exposure toroidal distribution of W from DiMES 74 along the radial center of the sample along with a fitted exponential function to the redeposited distribution. The two methods described above agree to within 20% for the erosion rate of the DiMES 74 W film, validating our measurement technique and indicating that essentially all the sputtered W is redeposited locally on the sample. A summary of the peak erosion rates and toroidal redeposition e-folding lengths for the various materials over the two exposure conditions is contained in Table 2.

The DiMES viewing visible camera, equipped with a CII line filter, indicated enhanced carbon production [Fig. 4(a)] on the leading edge of the downstream tile during the higher power DiMES 74 exposure. This was not observed for the previous ELM-free, low power

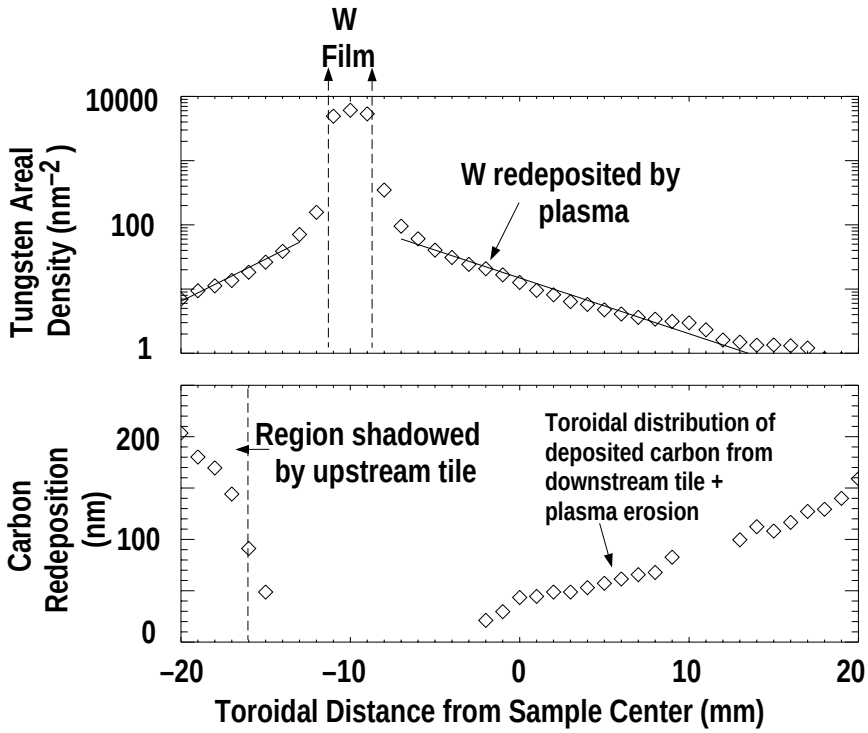

Fig. 3. (a) Toroidal distribution of tungsten areal concentration (from NRA) and carbon redposition (from RBS depth-marking) for DiMES 74. Regions with no carbon data are due to contaminating influence of metals on RBS depth-marking. (b) Radial profiles of heat flux and net carbon erosion for DiMES 70 and DiMES 74. (c) Radial profiles of ion flux, and beryllium and tungsten erosion rate for DiMES 74.

Table 2
Summary of Erosion Results from DiMES Experiments

Erosion Parameters		**Peak Erosion Rate (nm/s)**		**Toroidal redeposition e-folding length (cm)**	
Material	**Z**	**DiMES 70**	**DiMES 74***	**DiMES 70**	**DiMES 74**
Be	4	0.9	1.4	1.2	>1.5
C	6	3.6	16	-	-
V	23	0.5	-	0.7	-
Mo	42	0.3	-	0.5	-
W	74	0.1	0.45	0.25	0.4

exposures of DiMES 70&71. Dimensional checking of the sample showed that it was 0.1 mm shorter than the standard sample height, exposing a “leading edge” of nearly 0.3 mm at the downstream tile [Fig 1(b)]. RBS of the depth-marker [Fig. 3(a)] measures a toroidal variation in the net redeposition of carbon which suggests the following: carbon produced at the downstream tile is redeposited onto the DiMES sample at a rate which decreases linearly with

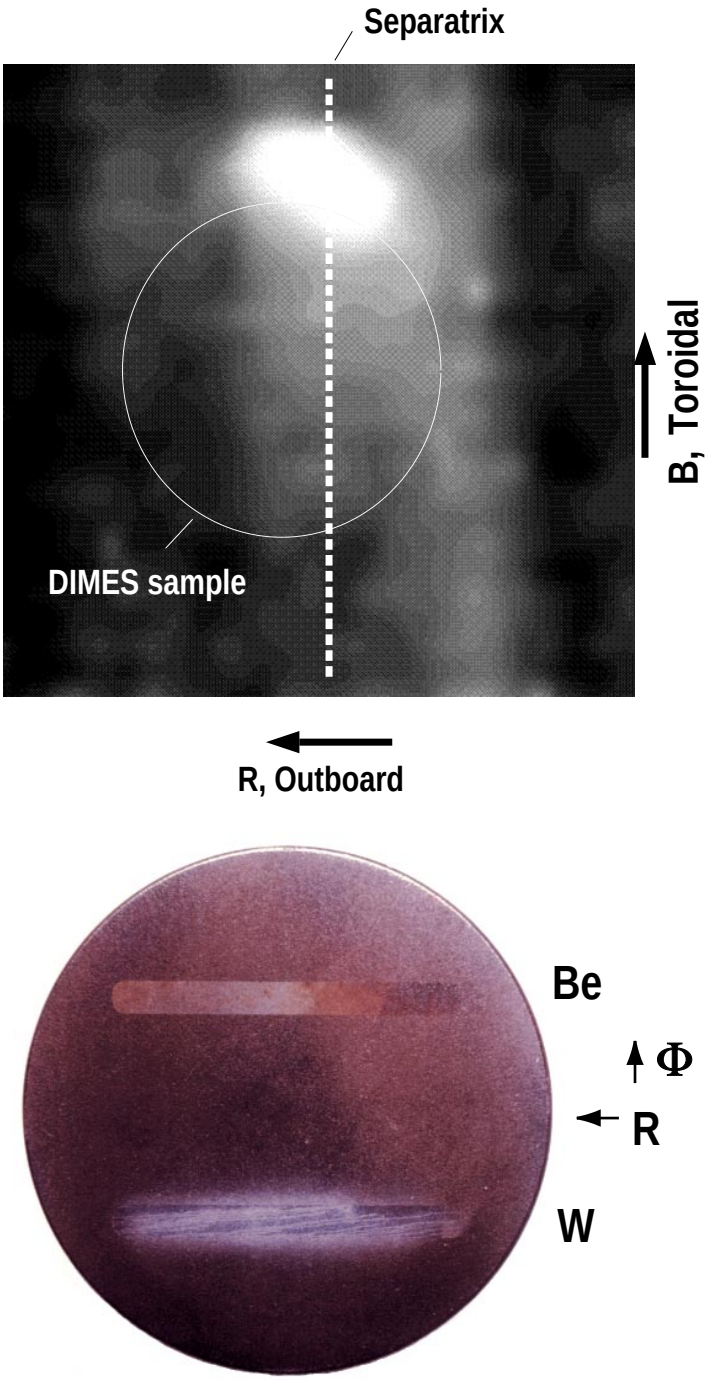

Fig. 4. (a) CII (5145 Å) camera image of DiMES 74 exposure. The camera is saturated at the bright spot on the downstream tile. (b) Post exposure photograph of DiMES 74. Note the darkening of the usually shiny Be film and the arc tracks on the W film.

toroidal distance from the tile, and the region of the sample which is shadowed from plasma erosion by the upstream tile indicates the background level of this redeposition. This is confirmed by the fact that the measured extent of the shadowed region (3–4 mm) matches the projected misalignment with the upstream tile along the incident field lines (i.e. d_{shadow}=0.1 mm/sin 2°=2.9 mm). Therefore, the calculation of plasma erosion rate of carbon

for DiMES 74 has been corrected for this anomalous redeposition. Also, contaminating layers of carbon were measured on the metal films of DiMES 74, up to 100 nm on the Be and up to 30 nm on the W. However, from the energy spectra of the RBS and NRA, it is determined that this layer's thickness is non-uniform and that sections of the metal remain uncovered. This is consistent with a source of redeposited carbon from the upstream tile which is incident on a rough metal surface at small angle. Additionally, visual inspection of the discoloration of the sample qualitatively shows a noticeable redeposition pattern which reveals the unexposed shadowed region and the carbon darkening of the Be film. Note that the apparent reduced scaling of the Be erosion rate with the increase in incident heat flux from DiMES 70 to DiMES 74 (Table 2) is highly questionable due to this carbon overlay. A future experiment will repeat these exposure conditions with improved sample alignment.

A post exposure photograph of the DiMES 74 sample indicated several radial arc tracks on the W film [Fig. 4(b)]. The CII line filtered visible camera shows arc-like behavior at the location of the W films only during the plasma breakdown of the initial exposure discharge. It is assumed that the arcs are due to the presence of an insulating layer of tungsten oxide (formed during the film deposition) which is quickly eroded away due to the arcs. However, this hypothesis remains speculative and we hope to confirm it during future experiments since frequent arcing could contribute significantly to erosion.

The diameter of the DiMES surface is on the order of the OSP flux's radial e-folding distance, allowing us to study the spatial dependence on erosion. Figure 5 compares the radial profiles of the heat flux and carbon erosion between DiMES 70 and DiMES 74. Note that both the heat flux and net erosion are broader for the ELMing plasma of DiMES 74. The increase in the absolute rate of erosion is larger than the increase in average heat flux. The radial stripes of the Be and W films on DiMES 74 provide the radial erosion profile of the metals. These erosion profiles closely follow the ion flux profile [Fig 6] as measured by a Langmuir probe.

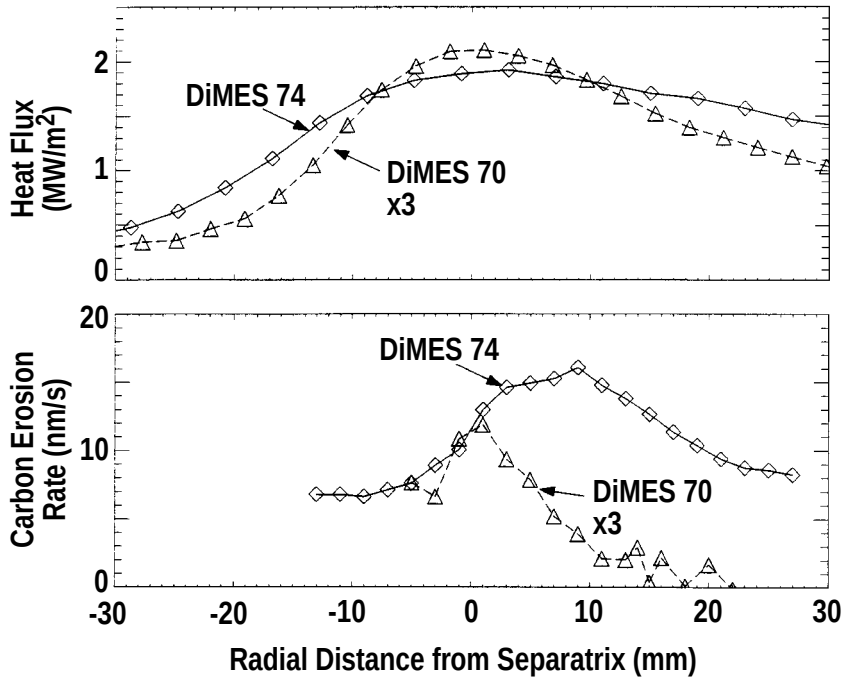

Fig. 5. (a) Radial profiles of heat flux and (b) net carbon erosion for DiMES 70 and DiMES 74.

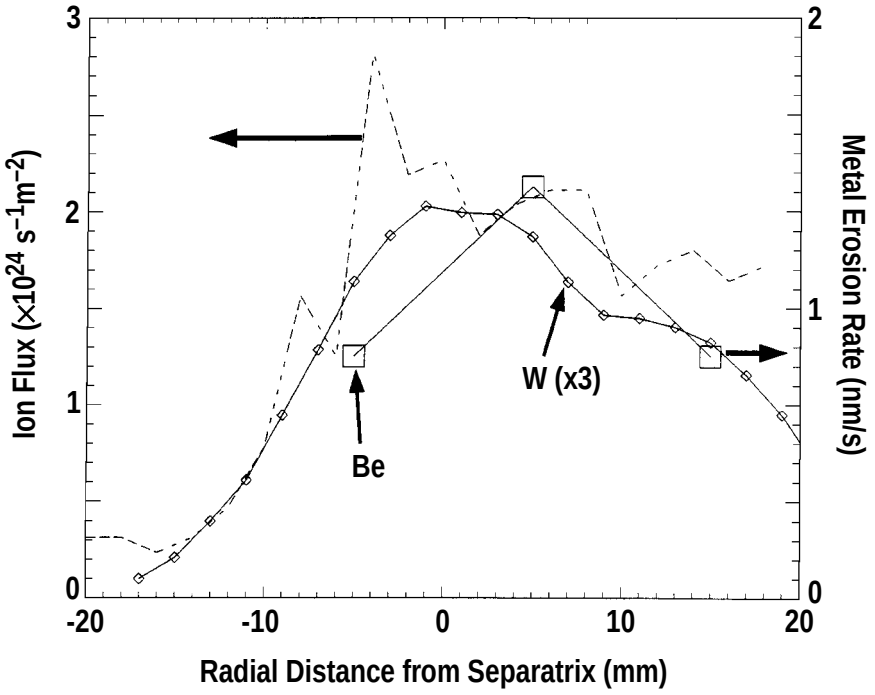

Fig. 6. Radial profiles of ion flux, and beryllium and tungsten erosion rate for DiMES 74.

3. DISCUSSION

One of the outstanding issues for the DiMES experiment is determining the validity of measuring the erosion rates of metal films in an "all-carbon" tokamak such as DIII–D. Certainly, the intrinsic carbon being deposited and re-eroded from the metallic surfaces perturbs the measurement to some extent. If the metal film is in a region of net carbon erosion, one should find some thin steady-state layer of carbon, while the metal is continually eroded at some reduced rate due to shielding from plasma by the carbon. This continual erosion is confirmed by the spectroscopy of the Be II line emission. The reduced rate of erosion seems evident from the comparison of Be and C erosion rates, for which the D^+ sputtering yields are comparable at these particle energies [4] and from more detailed calculation [5] we find that the measured Be erosion rate is 1/4 of the predicted rate. This matter is further complicated by the presence of enhanced redeposition as seen in DiMES 74. The presence of continual erosion of the Be, in an area of net carbon redeposition, suggests that surface roughness results in a very non-uniform layer of carbon on the metal.

The data shows a decrease of the net erosion rate, V_e, as the atomic number, A, of the metal film increases. Tabulated sputtering yields (Y) [4] of normal incident D^+ (no impurities or self-sputtering) for energies expected for these plasma conditions would yield a scaling of $Y_{D^+} \propto e^{-A/46}$. The measured net erosion rates actually show a weaker, yet comparable scaling of $V_e \propto e^{-A/77}$. The extrapolation of absolute erosion rates from these results (to say an all W or Be divertor) appears to be very difficult. However, the study of the the metal's transport under different plasma conditions remains valid. More sophisticated modeling is needed for the interpretation of the metal's absolute erosion rates, their mass scaling and the effect of the carbon.

It is apparent from the experimental results that the presence of ELMs has some effect on erosion. The net erosion of the carbon and the toroidal redeposition of the metals is broader in the presence of ELMs, suggesting enhanced transport of eroded materials. Also, if one simply assumes that the net erosion of carbon would scale linearly with the 3× increase in heat/ion flux between DiMES 70 and DiMES 74 then the >4× increase in net carbon erosion also suggests that ELMs have some detrimental effect on net losses. Future studies will attempt to isolate the effect of the ELMs by exposing samples to moderate (< 1 MW/m^2) heat flux comparable to DiMES 70, but in an ELMing discharge.

An earlier study of short exposure time DIII–D divertor erosion [1,6] provided data and analysis for both the overall carbon divertor, and a small tungsten spot. A similar comprehensive modeling effort is underway to analyze the new DiMES experiments, and a detailed paper on modeling of the transport and erosion is planned for the near future. Briefly, the analysis uses the WBC [7] and REDEP [8] impurity transport codes together with the

VFTRIM [5] sputtering codes. Code output is compared with measured erosion/redeposition profiles, and in the case of beryllium, with measured BeII 4673Å photon emission. For Be, Mo, and W, the computed redeposition profiles compare well to the data. The greater transport distances of Be compared to the high-Z metals are explained in terms of longer mean free paths for sputtered atom ionization, and by subsequent differences in ion transport. Photon emission calculations for Be also compare well to the data, namely within a factor of two, thereby tending to verify a wide variety of coupled models for plasma parameters, impurity transport, and atomic data.

The REDEP code was used to compute the erosion/redeposition profile for the entire divertor plate at the outer strike point region. REDEP results are shown in Fig. 7 for the

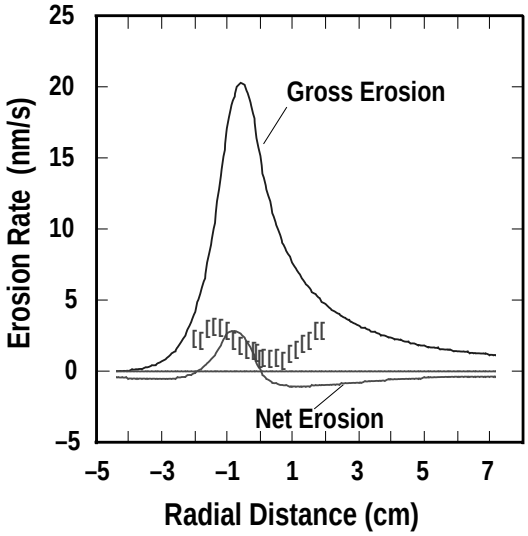

Fig. 7. Comparison of DiMES 70 carbon net erosion radial profile with REDEP calculations.

DiMES 71 experiment. (The code results are obtained for the entire outer strike point region while the data exists only for the ~5 cm wide probe region.) Inputs to the code are the measured plasma density, temperature, deuterium ion flux, and magnetic field profiles. This analysis is done for constant plasma parameters but takes into account strike point variations. The code results show both gross and net erosion rates peaking at the separatrix, a peak net rate of ~1/5 of the gross rate (i.e. 80% redeposition rate), and a region of net *growth* resulting from radial transfer of sputtered carbon. This redeposition rate is lower than the 90% value used for ITER lifetime calculations [9,6], but this relatively lower value is not unexpected in the low density/recycling, high temperature ELM-free H–mode used for the experiment. Considering the experimental uncertainty of ±10 nm in the erosion measurement (hence, ±0.7 nm/s) the code results compare reasonably well to the data. The code also predicts a core carbon contamination of ~1% resulting from outer strike point region erosion, and this too is consistent with measurements.

This validation of integrated PFC erosion codes with experimental tokamak erosion measurements is an important step in benchmarking these codes for use in designing large scale devices such as ITER. Also, the impact of the operating regime (i.e. attached vs. detached, high vs. low recycling, etc.) on issues such as particle transport, wall lifetimes [9], and other phenomenon such as co-redeposition [10], is needed and is being addressed in upcoming experiments.

4. CONCLUSIONS

DiMES has successfully measured the erosion rate of candidate PFC materials under real tokamak conditions in the DIII–D divertor. Preliminary scaling studies show that the erosion rate of the materials increases with heat flux and the introduction of ELMs. It is shown that small misalignments can produce anomalous carbon redeposition on the sample, making interpretation of erosion rates of both the carbon and the metals more suspect. Further experiments which correct this misalignment are needed to verify the current results. Nevertheless, DiMES is providing the necessary data for validating current erosion models.

REFERENCES

[1] C.P.C. Wong, R. Junge, R.D. Phelps, P.Politzer, F. Puhn, W.P West, R. Bastasz, D. Buchenauer, W. Hsu, J. Brooks, T. Hua, J. Nucl. Mater. 196-198 (1992) 871.

[2] R. Bastasz, W.R. Wampler, J.W. Cuthbertson, D. A. Buchenauer, N. Brooks, R. Junge, W.P. West, C.P.C. Wong, J. Nucl. Mater. 220-222 (1995) 310.

[3] W.R. Wampler, R. Bastasz, D. Buchenauer, D. Whyte, C.P.C. Wong, N.H. Brooks, W.P.West, "Erosion and Deposition of Metals and Carbon in the DIII-D Divertor," Proceedings of the Seventh International Conference on Fusion Reactor Materials, Obninsk, Russia, September 25-29, 1995, to be published in J. Nucl. Mater.

[4] C.F. Barnett, J.A. Ray, E. Ricci, M.I. Wilker, E.W. McDaniel, E.W. Thomas, H.B. Gilbody, Vol. II ORNL-5206 (1977).

[5] D.N. Ruzic, Nucl. Instr. and Meth. B47 (1990) 118.

[6] T. Q. Hua and J.N. Brooks, J. Nuc. Mat. 220-222 (1995) 342.

[7] J. N. Brooks, Phys. Fluids 8 (1990) 1858.

[8] J. N. Brooks, Nuc. Tech./Fusion 4 (1983) 33

[9] G. Janeschitz, K. Borrass, G. Federici, Y. Igitkhanov, a. Kukushkin, H.D. Pacher, G.W. Pacher, M. Sugihara, J. Nucl. Mater. 220-222 (1995) 73.

[10] J.N. Brooks, R. Causey, G. Frederici, D.N. Ruzic, these proceedings.

ACKNOWLEDGEMENTS

We acknowledge the technical support of T. Carlsness. We thank R. Isler for providing Be II excititation rates. This work was supported by the U.S. Department of Energy under contracts DE-AC04-94AL85000 (Sandia), W-31-109-Eng-38 (Argonne), and DE-AC03-89ER51114 (General Atomics).